JPP Journal of Pharmacy and Pharmacology
ROYAL PHARMACEUTICAL SOCIETY

JPP Journal of Pharmacy and Pharmacology

JPP 2011, 63: 342–351

Received June 21, 2010
Accepted October 19, 2010
DOI
10.1111/j.2042-7158.2010.01225.x
ISSN 0022-3573

Research Paper

Formulation development and systematic optimization of solid lipid nanoparticles of quercetin for improved brain delivery

Sanju Dhawan, Rishi Kapil and Bhupinder Singh

University Institute of Pharmaceutical Sciences (UGC Center of Advanced Studies), Panjab University, Chandigarh, India

Abstract

Objective This study aims at formulating solid lipid nanoparticles (SLNs) of quercetin, a natural flavonoid with established antioxidant activity, for intravenous administration in order to improve its permeation across the blood–brain barrier into the CNS, and eventually to improve the therapeutic efficacy of this molecule in Alzheimer's disease.

Methods The SLNs of quercetin were formulated using Compritol as the lipid and Tween 80 as the surfactant through a microemulsification technique, and optimized employing a 3^2 central composite design (CCD). Selection of the optimized SLN formulation, using brute-force methodology and overlay plots, was based on its efficiency of entrapping quercetin inside the lipophilic core, particle size, surface charge potential and ability of the SLNs to release the entrapped drug completely. The optimized formulation was subjected to various in-vivo behavioral and biochemical studies in Wistar rats.

Key findings The optimized formulation exhibited a particle size of less than 200 nm, 85.73% drug entrapment efficiency and a zeta potential of 21.05 mV. In all the in-vivo behavioral and biochemical experiments, the rats treated with SLN-encapsulated quercetin showed markedly better memory-retention vis-à-vis test and pure quercetin-treated rats.

Conclusions The studies demonstrated successful targeting of the potent natural antioxidant, quercetin, to brain as a novel strategy having significant therapeutic potential to treat Alzheimer's disease.

Keywords Alzheimer's disease; blood brain barrier; design of experiments (DoE); flavonoids; memory enhancement

Introduction

Alzheimer's disease is a progressive age-related neurodegenerative disorder with distinct neuropathological features. About three percent of world's population between the age of 65 to 74 years, and nearly half of the population aged 85 years or older, is inflicted with this disease.[1,2] In this condition, amyloid-beta (Aβ) accumulates as plaques in the extracellular space of the gray matter and in artery walls as cerebral amyloid angiopathy, and tau protein accumulates as neurofibrillary tangles within neurons. The other neuropathological features of Alzheimer's disease include neuronal loss, synaptic depletion, Hirano bodies and granulovacuolar degeneration.[3] Various strategies have been developed to prevent or mitigate the progression of Alzheimer's disease. Despite the medical need for an effective therapeutic treatment, the pace of progress towards this goal has been painstakingly slow. Current therapies for Alzheimer's disease, such as the cholinesterase inhibitors and NMDA receptor antagonists, provide moderate symptomatic delay of the disease without arresting the disease progression. Accordingly, newer approaches for the disease management are the acute need of the hour.

Flavonoids, a class of secondary plant metabolites, have recently gained wide attention because of their antioxidant, anti-inflammatory, antiplatelet and other beneficial properties.[4–6] Quercetin, a natural flavonoid molecule, has a long history of consumption as a part of the human diet, and is found in fruits, vegetables, wine and tea. It has been postulated to act as a novel neuroprotectant by mitigating the increased levels of reactive oxygen species produced by normal mitochondrial activity, which accelerate the neurodegenerative processes of Alzheimer's disease.[7,8] In this regard, quercetin has been documented to be a more potent antioxidant and radical scavenger than vitamin C, vitamin E and

Correspondence: Bhupinder S. Bhoop, University Institute of Pharmaceutical Sciences, UGC Centre of Advanced Studies, Dean, Alumni Relations, Panjab University, Chandigarh 160 014, India.
E-mail: bsbhoop@yahoo.com, bsbhoop@pu.ac.in

β-carotene.[9] Besides, this flavonoid has been shown to improve spatial learning and memory in D-galactose-treated aging in mice.[10] These valuable effects of quercetin, however, are thwarted because of its limited penetration into the CNS. Although a few attempts have been made to formulate various drug delivery systems of quercetin-like microemulsions[11] and nanoparticles,[12] no studies have been reported on enhancing the brain permeability of the drug. Accordingly, this investigation aimed to formulate solid lipid nanoparticles (SLNs) of quercetin for intravenous administration to improve its permeation across the blood–brain barrier into the CNS,[13,14] and eventually, to improve its therapeutic efficacy in Alzheimer's disease.

Materials and Methods

Materials

Quercetin was purchased from M/s Sisco Research Laboratories (Maharashtra, India). Compritol 888 ATO was a gift from M/s Colorcon Asia Pvt. Ltd (Goa, India), while Tween 80 was procured from M/s SD Fine Chemicals Ltd (Maharashtra, India). Aluminium chloride was purchased from Central Drug House Pvt. Ltd (New Delhi, India). All other reagents were of analytical grade and were used as received.

Formulation of solid lipid nanoparticles

Compritol (quantity varied as per the experimental design) was heated to its melting point (i.e. 70–75°C) and quercetin (50 mg) was dispersed thoroughly in the molten lipid to form a homogenous dispersion. Water (6 g) and Tween 80 (quantity varied as per the experimental design) were mixed separately and heated to the same temperature as the lipid dispersion. After the two phases became isothermal, the aqueous phase was poured into the lipid phase under magnetic stirring to obtain a clear homogenous microemulsion, which was then poured into 100 ml of cold water, and stirred at 1500 rev/min in an ice-bath for 40 min to obtain a fine dispersion of the SLNs. The dispersion was freeze-dried using a lyophilizer (Alpha, 2–4 LD plus; Martin Christ, Osterode am Harz, Germany) to obtain a fine powder. The lyophilized powder was subsequently re-dispersed in 1% Tween 80 (v/v) solution or normal saline solution (0.9% w/v NaCl) to obtain Tween 80 coated or uncoated particles, respectively. Various SLN formulations were prepared employing varying concentrations of Compritol and Tween 80, keeping the amount of quercetin constant. By studying the total drug content, particle size, drug release profile and drug entrapment efficiency of the above-mentioned formulations, limits and ranges for Compritol and Tween 80 were set for the subsequent optimization studies using a two-factor central composite design (CCD).

Experimental design

A CCD (with $\alpha = 1$) using three levels each of the two factors[15] *viz* polymer X (i.e. Compritol) and polymer Y (i.e. Tween 80), was adopted for further investigations as required by the design, and the factor levels were suitably coded. Table 1 summarizes an account of the 13 experimental runs studied employing a total of nine formulations. All the studies were conducted in triplicate, and the formulation at central point (0, 0) was studied in quintuplicate.

Table 1 Composition of various solid lipid nanoparticle formulations prepared as per the experimental design

Formulation code	Trial No.	Coded factor levels	
		X_1	X_2
SA	1	−1	−1
SB	2	−1	0
SC	3	−1	1
SD	4	0	−1
SE	5	0	0
SF	6	0	1
SG	7	1	−1
SH	8	1	0
SI	9	1	1
Translation of coded levels in actual units			
Coded Level		−1	0	1
X_1: Compritol (mg)		200	400	600
X_2: Tween 80 (g)		4	6	8

In-vitro drug release

Drug release studies from SLNs were performed in the solvent mixture of phosphate-buffered saline (pH 7.4) and methanol (80 : 20, v/v) using the dialysis bag method.[16] Quercetin-SLN suspension equivalent to 2 mg of drug was placed in the bags, which were then suspended with the help of a thread in a conical flask containing 200 ml of dissolution medium (37 ± 1°C) stirred at 100 rev/min. A sample of the dissolution medium (2 ml) was periodically withdrawn at each time interval and immediately replaced with the same volume of fresh dissolution medium to maintain the sink condition. An analogous study was also preformed with an equal amount of pure quercetin in its solution. Quercetin in the sample solution was analysed at 257 nm by a previously validated UV-Vis spectrophotometric method taking $E_{1cm}^{1\%}$ as 663 and molar extinction coefficient, ε, as 20022.6.

The raw data obtained from the in-vitro dissolution study were analysed using ZOREL software.[17] This software has in-built provisions for applying the correction factor for volume and drug losses during sampling,[18] calculating the values of percent drug released, rate of drug release and log fraction released at varied times. Using the software, the values of kinetic constant (k) and diffusional release exponent (n) was determined. Based on the phenomenological analysis, the type of release, whether Fickian, non-Fickian (anomalous) or zero-order, was predicted.

Drug entrapment efficiency

Drug entrapment efficiency was determined using the dialysis membrane method by allowing the unentrapped drug to diffuse through the membrane placed inside the sink medium (i.e. methanol).[19] The unentrapped drug (i.e. drug diffused out of the membrane) was quantified by analysing it spectrophotometrically at 257 nm using a previously validated method taking $E_{1cm}^{1\%}$ as 652 and molar extinction coefficient, ε, as 19690.4.

Particle size determination

The particle size distribution of all the nine SLN dispersions was observed using a Mastersizer 2000 (Malvern Instruments Ltd, Worcestershire, UK) to access the size range and uniformity of particle size distribution in the formulation.

Zeta potential determination

The zeta potential of all the nine formulations was determined using a Zetasizer (Malvern Instruments Ltd, Worcestershire, UK). The instrument was operated at a constant temperature of 25°C using a clear disposable zeta cell.

Optimization data analysis

The response variables considered for systematic optimization were particle size, drug entrapment efficiency, amount of drug release in 20 h (Rel_{20}) and zeta potential. Design Expert software ver. 6.0 (Stat-Ease, Minneapolis, MN, USA) was employed to fit full second-order polynomial equations with added interaction terms to correlate the studied responses with the examined variables. The prognosis of optimum formulations was conducted in two stages: first, a feasible space was located and second, an exhaustive grid search was conducted to predict the possible solutions. The optimized formulation was also located by overlay plot option of the Design Expert software, while 'trading off' of the responses.

Electron microscopic examination

The optimized formulation was viewed under a transmission emission microscope (TEM, H7500; Hitachi, Tokyo, Japan) to observe the surface morphology of the particles.

Stability studies

The SLN samples were stored in a refrigerator (i.e. at 2–8°C) and at 25°C/65% RH to assess the storage stability of optimized formulation and ascertain the storage conditions. Samples were periodically withdrawn at monthly intervals for four months and examined for their particle size, entrapment efficiency and drug release characteristics.

In-vivo studies

Animals

Male Wistar rats, 180–200 g, procured from Central Animal House, Panjab University, Chandigarh were used in the investigation. The protocol was approved by the Institutional Animal Ethics Committee and was carried out in accordance with the Indian National Science Academy guidelines for the use and care of animals.

Drugs and treatment schedule

Aluminium chloride solution and the optimized quercetin SLNs were freshly prepared at the beginning of each experiment. For oral administration, aluminium chloride was dissolved in drinking water and for intravenous administration, lyophilized SLNs were dispersed in normal saline or 1% v/v Tween 80 solution. The dose of quercetin for rats was calculated employing Equation 1, taking K_m factor for humans and rats as 37 and 6, respectively.[20]

$$Human\ Dose = Animal\ Dose \times \frac{Animal\ K_m}{Human\ K_m} \quad (1)$$

Before experimentation, rats were randomized into the following seven groups, each group consisting of four rats.

Group I	Naïve rats
Group II	Control (distilled water p.o. + vehicle for quercetin i.v.)
Group III	Aluminium chloride (100 mg/kg p.o.)
Group IV	Quercetin (4.41 mg/kg i.v.) dissolved in 70 : 30 v/v mixture of PEG 200 and DMSO
Group V	Aluminium chloride (100 mg/kg p.o.) + quercetin (4.41 mg/kg i.v.) dissolved in vehicle
Group VI	Aluminium chloride (100 mg/kg p.o.) + Tween 80 coated SLNs i.v. (equivalent to 4.41 mg/kg of quercetin)
Group VII	Aluminium chloride (100 mg/kg p.o.) + uncoated SLNs i.v. (equivalent to 4.41 mg/kg of quercetin)

The study was carried out for a period of eight weeks.

Spatial navigation task

The acquisition and retention of a spatial navigation task was evaluated using a Morris water maze.[21] Rats were trained to swim to a visible platform in a circular water-pool (180 cm in diameter and 60 cm in height) located in a test room.[22] The rats received a training session consisting of four trials on day 52, 53, 54 and 55. The latency to find the escape platform was recorded to a maximum of 90 s. Twenty-four hours after the last training (i.e. on day 56), the rats were released randomly at one of the edges facing the wall of the pool and tested for retention of response.

Elevated plus maze paradigm

The elevated plus maze consisted of two opposite black open arms (50 cm × 10 cm), crossed with two closed walls of the same dimensions with 40 cm high walls.[21] Acquisition of memory by the rats was tested on the 44th day from the start of aluminium chloride administration. The time taken by the rat to move from the open arm to the closed arm was recorded as the initial transfer latency (ITL). Rats were allowed to explore the maze for 20 s after recording the ITL and were made to return to the home cages. If the rat did not enter the enclosed arm within 90 s, it was pushed back into one of the enclosed arms and the ITL was recorded as 90 s. Retention of memory was assessed by placing the rat in an open arm. The retention latency was noted on day 45 and day 56, termed as the first retention transfer latency (1st RTL) and second retention transfer latency (2nd RTL), respectively.[23]

Assessment of gross behavioral activity

Gross behavioral activity was observed using digital photoactometer at the end of every 15 days for a total of 60 days after the initiation of aluminium chloride treatment.[24]

Biochemical assessment

Biochemical tests were carried out 24 h after the last behavioral test (i.e. on 57th day). Rats were sacrificed by decapitation and the brains were removed and rinsed with ice-cold isotonic saline. Brain tissue samples were then homogenized with 10 times (w/v) ice-cold 0.1 M phosphate buffer (pH 7.4). The homogenate was centrifuged at 4000 rev/min for 15 min

and samples of supernatant were used for estimating lipid peroxidation, glutathione levels and nitrite levels in brain tissue.[21,25,26]

Statistical analysis

The behavioral and biochemical assessment data were analysed by one-way analysis of variance, followed by one-tailed Student's *t*-test.[27] $P \leq 0.05$ was considered as statistically significant.

Results

In-vitro drug release

The in-vitro drug release profile of the formulations, prepared as per the experimental design, is depicted in Figure 1. Formulations SA, SB, SC and SG exhibited a high burst release. A summary of the dissolution parameters (Table 2) shows that the value of diffusional release constant, n, varies between 0.2823 and 0.5649, indicating that the type of drug release varies between Fickian and non-Fickian behaviour. Quercetin in its solution form, however, exhibited an 'n' value of 0.7329, indicating non-Fickian behaviour. The values of the kinetic constant, k, showed a declining trend with an increase in the concentration of Tween 80 at all the levels of Compritol studied. Maximum extent of drug release was observed at the lowest levels of both the ingredients.

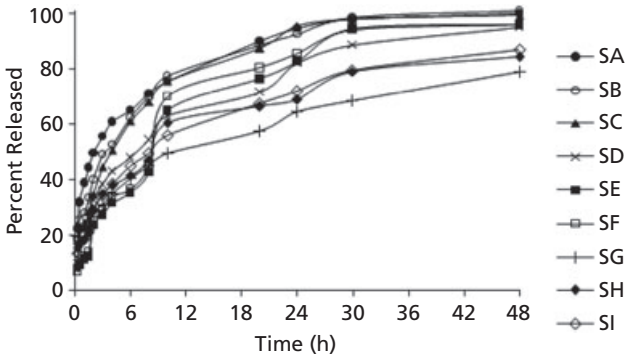

Figure 1 In-vitro drug release profiles of formulations prepared as per the experimental design.

Table 2 Dissolution parameters of various formulations prepared as per the experimental design

Code	Formulation composition		Release exponent (n)	Kinetic constant (k)	Drug released till 20 h (Rel_{20}, %)
	Compritol (mg)	Tween 80 (g)			
SA	200	4	0.2823	0.3783	90.14
SB	200	6	0.3445	0.3129	88.77
SC	200	8	0.3828	0.2770	87.41
SD	400	4	0.3844	0.2395	71.70
SE	400	6	0.5413	0.1422	76.49
SF	400	8	0.5649	0.1421	80.53
SG	600	4	0.2869	0.2482	57.64
SH	600	6	0.3667	0.2222	66.63
SI	600	8	0.3759	0.2203	67.77
Pure drug in its solution			0.7329	0.8469	–

Drug entrapment, particle size and zeta potential determination

The values of percent drug entrapment, particle size and zeta potential of the formulations, prepared as the experimental design are shown in Table 3. Formulations SA, SB, SC and SG exhibited low drug entrapment values. Formulations SB, SC and SG were observed to possess high mean values of particle size (i.e. >2 μm) too.

Exploration of polymer mechanism using response surface methodology (RSM)

In all, eight coefficients (β_0–β_7) were calculated, with β_0 representing the intercept, and β_3–β_7 representing the coefficients of various quadratic and interaction terms (Equation 2).

$$Y = \beta_o + \beta_1 X_1 + \beta_2 \chi_2 + \beta_3 X_1 \chi_2 + \beta_4 X_1^2 + \beta_5 X_2^2 + \beta_6 X_1 X_2^2 + \beta_7 X_2 X_1^2 \quad (2)$$

Table 4 lists the coefficient values of polynomial equations along with their statistical parameters for the studied response variables. To study the effect of the two independent factors (i.e. Compritol and Tween 80), 3-D response surface graphs and 2-D contour graphs were constructed.

At lower levels of Tween 80, there was a marginal decreasing trend in the values of particle size, as the amount of Compritol increased from lower to intermediate levels (Figure 2). Tween 80 exhibited significant positive influence on particle size at lower levels of Compritol, the effect being slightly negative but less significant at higher levels of the lipid. The slanting lines of the corresponding contour plot also confirmed the same.

As depicted in Figure 3, entrapment efficiency showed an umbrella-like asymptotic curve with an increased concentration of Compritol (i.e. the value of entrapment efficiency first increases nonlinearly and then decreases marginally with an increase in the concentration of Compritol). The corresponding contour plot depicted highest entrapment efficiency at the intermediate levels of both the polymers.

Figure 4 depicts a linear decline in the value of Rel_{20} with an increase in the concentration of Compritol. However,

Table 3 Particle size, percent drug entrapment and zeta potential of solid lipid nanoparticle formulations prepared as per the experimental design

Formulation	Size (μm)	Entrapment (%)	Zeta potential (mV)
SA	0.94	59.41	–12.3
SB	2.23	65.59	–9.82
SC	4.62	69.71	–5.13
SD	0.229	74.12	–23.6
SE	0.152	87.65	–20.7
SF	0.45	92.65	–11.2
SG	2.39	63.52	–8.82
SH	1.34	81.12	–17.3
SI	0.42	85.88	–15.9

Table 4 Coefficient values of polynomial equations with their statistical parameters for the studied response variables

Coefficient code	Size	Entrapment	Rel_{20}	Zeta potential
β_0	+0.14	+87.58	+76.71	+20.66
β_1	−0.45***	+7.77***	−11.07***	+3.74***
β_2	+0.11*	+9.27***	+4.41***	−6.20***
β_3	+1.69***	−14.03***	+0.44	−7.01***
β_4	+0.25***	−4.00***	−1.14*	−3.17***
β_5	−1.41***	+3.02***	+3.22***	+3.56***
β_6	+0.32***	−1.10**	−2.57**	+6.18***
β_7	−0.24**	−2.70***	−1.97*	−1.92***
r^2	0.9995	0.9999	0.9983	0.9999
Adj r^2	0.9989	0.9997	0.9983	0.9997
Pred r^2	0.9463	0.9847	0.9834	0.9851
CV	4.33	0.25	0.77	0.65
Model significance	$P < 0.0001$	$P < 0.0001$	$P < 0.0001$	$P < 0.0001$

*$P < 0.05$; **$P < 0.01$; ***$P < 0.001$.

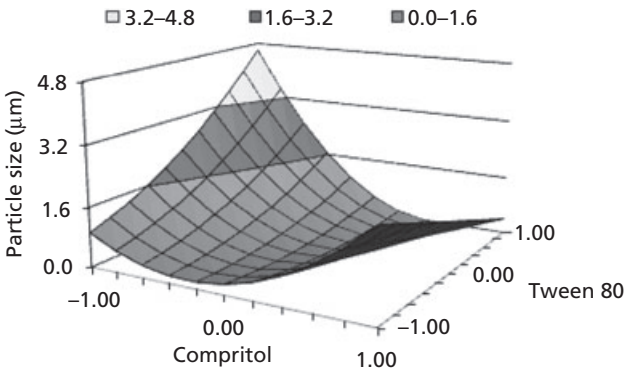

Figure 2 Response surface graph showing the influence of Compritol and Tween 80 on particle size of solid lipid nanoparticles.

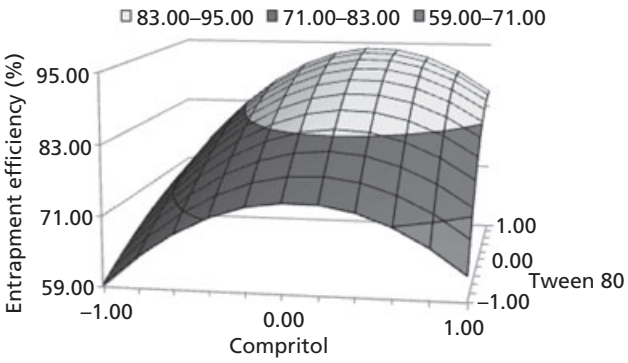

Figure 3 Response surface graph showing the influence of Compritol and Tween 80 on entrapment efficiency of solid lipid nanoparticles.

Tween 80 did not seem to exert any significant effect on the values of Rel_{20} barring a slight increase at the higher levels of Compritol.

At low levels of Tween 80, a characteristic inverted 'U'-type trend increase in the values of zeta potential with a shift from lower to intermediate levels of Compritol was observed (Figure 5). However, a somewhat declining trend was observed at lower levels of Compritol. The curved lines of the corresponding contour plot depicted the highest value of zeta potential at intermediate levels of both the polymers.

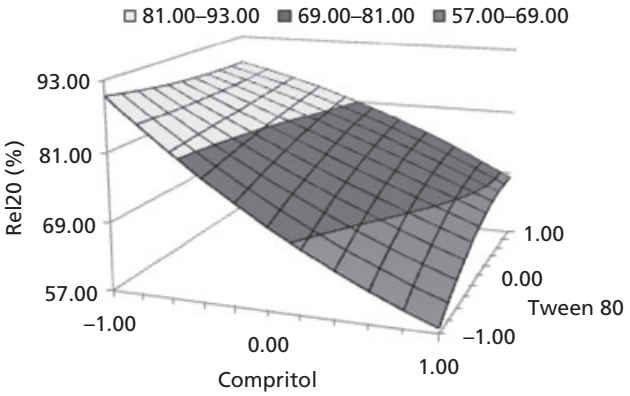

Figure 4 Response surface graph showing the influence of Compritol and Tween 80 on Rel_{20} of solid lipid nanoparticles.

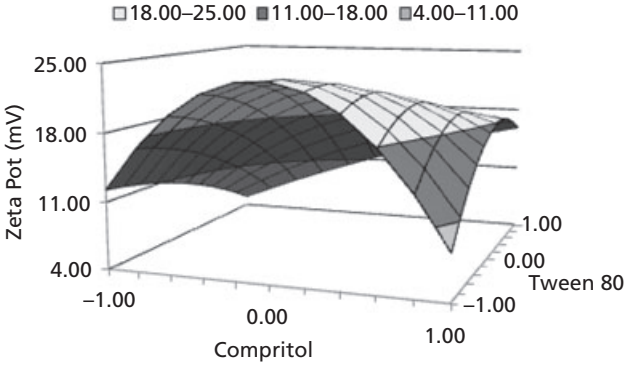

Figure 5 Response surface graph showing the influence of Compritol and Tween 80 on zeta potential of solid lipid nanoparticles.

Two feasible regions were selected as per the following criteria:

$$\text{Size} < 300\ \text{nm};\quad \text{entrapment} > 81\%;$$
$$Rel_{20} > 74.5\%;\quad \text{zeta potential} > 15.5\ \text{mV}$$

An exhaustive grid search was then conducted within the selected feasible regions to further narrow-down the region of optimal formulation. Based on the final grid search, the formulation containing 384 mg of Compritol and 5.76 g of Tween 80 was selected as the optimal SLN formulation. The selection of the optimum formulation was based on minimization of particle size below 200 nm to facilitate brain targeting,[28] maximization of entrapment efficiency and Rel_{20}, and maximization of zeta potential to avoid coalescence of particles. The said formulation exhibited a particle size of 159 nm, entrapment efficiency of 85.73%, Rel_{20} of 77.09% and zeta potential of 21.05 mV.

To validate the search for optimal formulation, a region was marked in the overlay plot (Figure 6) corresponding to

optima, and corresponding responses were predicted for the optima. In this investigation, the optima searched by brute-force methodology (feasibility and grid search) and overlay plot came out to be quite identical.

Electron microscopic examination

The TEM images of the optimal SLN formulation are shown in Figure 7. As depicted in the image, the particles possessed uniform shape. The size of all particles was found to be less than 200 nm.

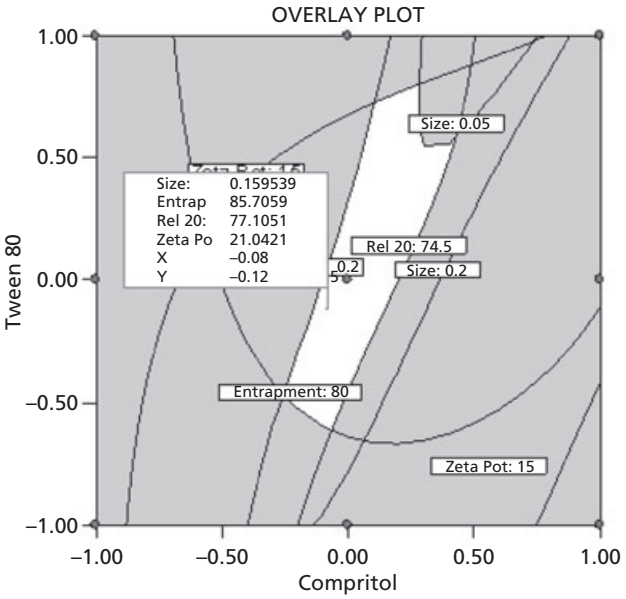

Figure 6 Overlay plot showing the location of optimized formulation.

Stability studies

The formulation stored in refrigerated conditions did not exhibit any significant change in its particle size, drug entrapment efficiency and drug release characteristics after four months of storage. The formulation stored at 25°C/65% RH, however, exhibited increased particle size from the erstwhile nanometer range to micrometer range along with a significant decrease in drug entrapment efficiency. The results of the stability studies are summarized in Table 5.

In-vivo studies

Spatial navigation task

In the spatial navigation task, the naïve, control and quercetin *per se* group of rats quickly learned to swim directly to the platform in the Morris water maze. Aluminium chloride-treated rats showed an initial increase in escape latency, which declined with continued training during the acquisition of spatial navigation task. The rats that received pure quercetin along with aluminium chloride showed slight improvement in their behaviour. In contrast, concomitant administration of quercetin formulated as SLNs with aluminium chloride significantly ($P < 0.00001$) decreased the time taken to reach the platform in the pre-trained rats as compared with aluminium chloride-treated rats (Figure 8).

Elevated plus maze paradigm

In the elevated plus maze task, mean ITL on day 20 for each rat was relatively stable and showed no significant variation. All the rats entered the closed arm within 90 s. Following

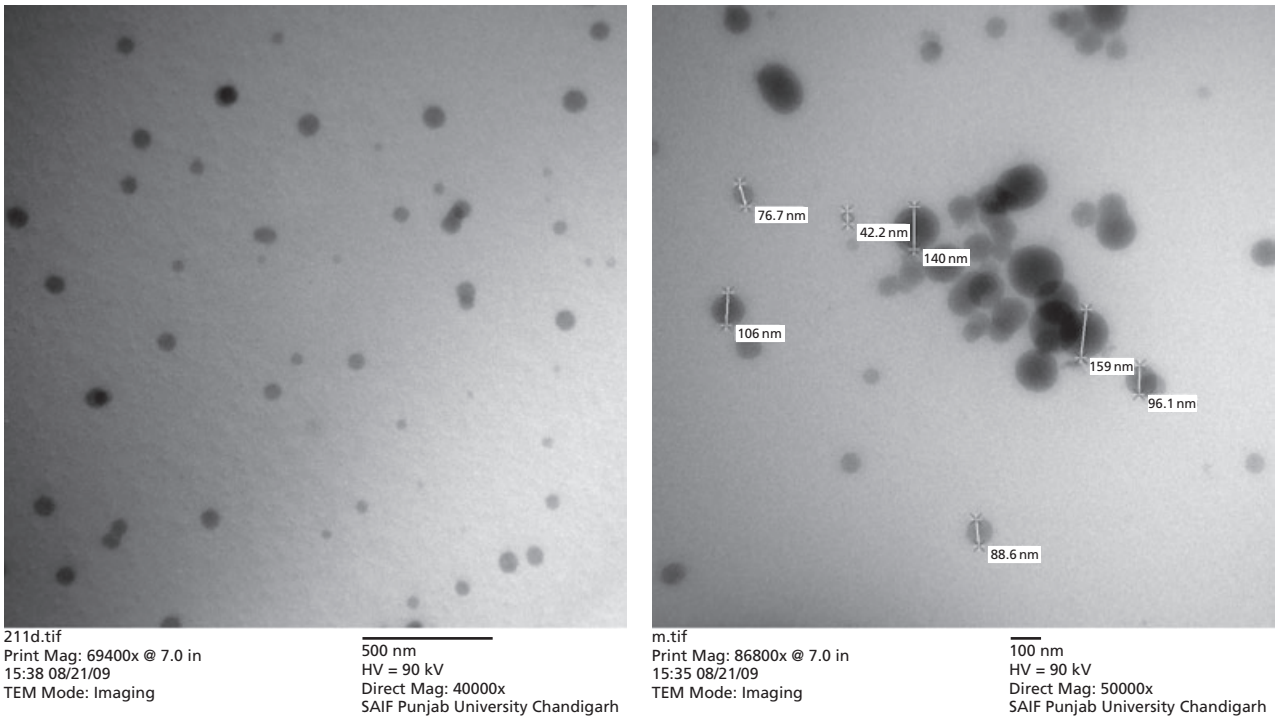

Figure 7 Transmission electron microscopic images of the optimized formulation.

Table 5 Various parameters of the optimized formulation analysed at different time points during stability studies

Parameters	Stability time points (months)									
	0	1	2	3	4	0	1	2	3	4
	Refrigerated conditions					25°C/ 65% RH				
Particle size (nm)	153	170	181	184	190	153	1231	1681	1833	1842
Entrapment efficiency (%)	88.53	86.17	85.58	85.29	84.72	88.53	64.11	57.64	55.31	48.92
Rel_{20} (%)	78.63	77.57	77.21	76.84	76.62	78.63	86.52	89.71	90.34	92.59

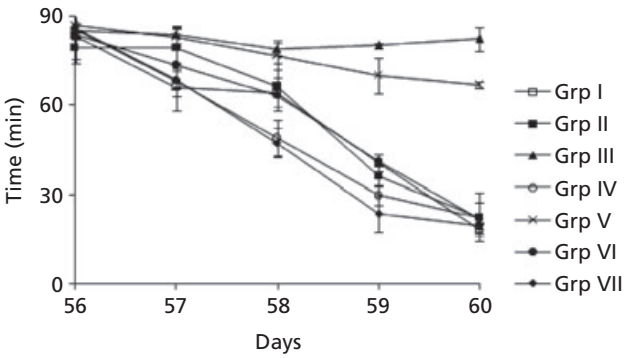

Figure 8 Comparison of memory retention in various groups of rats using spatial navigation task. The values are depicted as mean ± SD ($n = 4$).

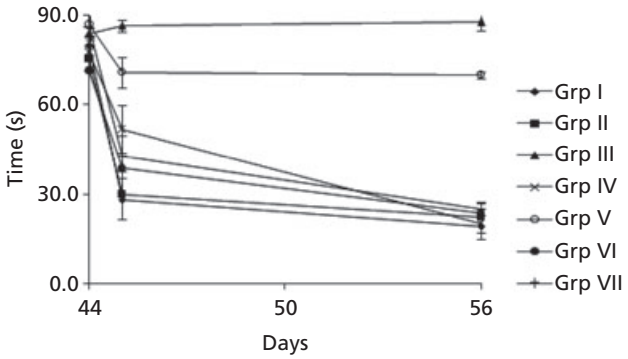

Figure 9 Comparison of memory retention in various groups of rats using elevated plus maze paradigm. The values are depicted as mean ± SD ($n = 4$).

training, naïve, control and quercetin *per se* treated rats entered the closed arm quickly and mean retention transfer latencies (1st RTL and 2nd RTL) to enter closed arm on days 45 and 56 were shorter as compared with the ITL on day 44 for each group, respectively. In contrast, aluminium chloride-treated rats performed poorly throughout the experiment and did not show any change in the mean retention transfer latencies on days 45 and 56 as compared with pre-training latency on day 44, demonstrating that chronic administration of aluminium chloride induced marked memory impairment. Chronic administration of quercetin-loaded SLNs following aluminium chloride administration significantly decreased the mean retention latencies on days 45 ($P < 0.005$) and 56 ($P < 0.0001$) as compared with pure quercetin administration, indicating enhancement of the anti-Alzheimer's potential of quercetin on being formulated as SLNs. The results are depicted graphically in Figure 9.

Assessment of gross behavioral activity

In this series of experiments, the gross behavioral activity as measured by the mean scores of locomotor activity for each rat was relatively stable and showed no significant variation. The mean scores in naïve, control and aluminium chloride-treated rats did not show much change. Chronic administration of quercetin or SLNs of quercetin also had no significant effect on the locomotor activity as compared with naïve rats throughout the study period ($P > 0.1$).

Biochemical estimation

Chronic administration of aluminium chloride caused marked increase in free radical generation and significant rise in brain MDA, nitrite levels and decrease in reduced GSH levels as compared with naïve rats. Further, there was less alteration in the brain MDA level, nitrite level and reduced GSH level due to quercetin *per se* treatment as compared with naïve rats. However, simultaneous chronic quercetin-loaded SLN administration to aluminium chloride-treated rats significantly prevented ($P < 0.00001$) the increase in MDA, nitrite levels and depletion of reduced GSH (Table 6).

Table 6 Percent changes in brain malondialdehyde, nitrite and glutathione levels in various groups of rats vis-à-vis naïve rats

Animal groups	% Decrease in brain glutathione levels	% Increase in brain MDA levels	% increase in brain nitrite levels
Grp II	2.08 ± 1.91	8.25 ± 3.76	5.07 ± 2.36
Grp III	90.27 ± 23.87	882.13 ± 102.33	377.79 ± 67.88
Grp IV	11.67 ± 3.28	3.43 ± 1.76	6.97 ± 2.32
Grp V	86.02 ± 21.44	243.64 ± 43.87	233.50 ± 62.83
Grp VI	18.51 ± 11.91	17.18 ± 12.49	26.14 ± 12.37
Grp VII	16.27 ± 10.56	25.08 ± 10.35	16.24 ± 6.83

MDA, Malondialdehyde. Data are means ± SD

Discussion

SLNs are considered to be safe and effective carriers for a variety of applications like topical delivery of drugs,[29] pulmonary delivery[30] and enhancement of efficacy of anticancer drugs.[31] Their potential in brain targeting of therapeutic moieties is well established and widely reported in literature.[13,28,32]

Among stearic acid, Compritol and palmitic acid, Compritol was selected as the lipidic carrier owing to better drug entrapment efficiency and lower particle size of the SLNs prepared using Compritol. Among Brij 78, Tween 80, Tween 40 and Lutrol F-68, Tween 80 was selected as the surfactant owing to better acceptability of Tween 80 through the intravenous route, better drug entrapment efficiency and ability to target SLNs to brain owing to its hydrophilic nature. Besides, earlier studies have also demonstrated successful formulation of SLNs using Compritol as the lipidic carrier and Tween 80 as the surfactant.[33,34]

A CCD for two factors at three levels with $\alpha = 1$, equivalent to 3^2 factorial design (FD), was chosen as the experimental design. This is considered to be an effective second-order experimental design associated with a minimum number of experiments to estimate the influence of individual variables (main effects) and their second-order effects[15,35] and has been successfully implemented for systematic optimization of various drug delivery systems.[15,36–38] Further, this design has an added advantage of determining the quadratic response surface, not estimable using an FD at two levels.[39–41]

The high burst release observed with Formulations SA, SB and SC can be attributed to the presence of un-entrapped drug present on the surface of SLNs, as the amount of lipid used in these formulations was not sufficient to entrap the drug completely. Further, Formulation SG also exhibited a high burst release, which can again be attributed to the presence of un-entrapped drug as the amount of surfactant used in this formulation was too low to support the high quantity of Compritol. The results of drug release pattern are in consonance with earlier findings where a combination of Fickian and quasi-Fickian behaviours has been proposed for release of drugs from SLNs.[42,43] The values of k indicated a significant change in the polymer characteristics with change in the surfactant levels. Further, the low percent drug entrapment observed in Formulations SA, SB, SC and SG can also be attributed to the reasons mentioned above. The large particle size of SB and SC was observed due to the presence of an excess of Tween 80 compared with the low amount of lipid in these formulations. This excess of hydrophilic surfactant made the particles coalesce, which was further supported by the low zeta potential of these formulations.[44,45] The high particle size of Formulation SG can also be attributed to the low zeta potential.

Quite high values of R^2 of the MLRA coefficients for all four responses, ranging between 0.9983 and 0.9999, vouch high prognostic ability of the RSM polynomials. Statistically, the models for all the response variables were found to be highly significant using analysis of variance ($P \leq 0.0001$). The closeness in the magnitudes of adjusted r^2 and predicted r^2 to the actual model r^2, and the low coefficient of variance also suggest high goodness of fit of the postulated model to the data. The response surface and contour plots for particle size confirmed that to attain a particular particle size, higher levels of Tween 80 have to be complemented with lower levels of Compritol and vice-versa. Further the 'U'-type response surface curve depicting a curvilinear increase in the values of zeta potential with an increase in the concentration of Tween 80 unequivocally vouch for the presence of some type of interaction between the lipid and the surfactant. The optimum formulation searched by brute-force methodology and overlay plots came out to be identical indisputably vouching the efficient location of optimal formulation.

TEM studies of the optimized formulation showed uniform particle shape and a size of <200 nm, which is considered imperative for ideal drug transport into the CNS.[28] Stability studies indicate that storage at room temperature (i.e. 25°C) leads to decreased entrapment and increased particle size attributable to coalescence of the erstwhile nanoparticulate system to microparticulate one. Thus refrigeration (i.e. 2–8°C) was found to be the preferred storage condition for SLNs. Earlier findings have also indicated that 4°C is the best storage temperature for SLNs.[28,46,47]

Experimentally, it has been demonstrated that chronic exposure to aluminium not only causes neurological signs that mimic progressive neurodegeneration but also results in neurofilamentous changes in the hippocampus, cerebral cortex, brain stem and spinal cord and biochemical changes which are seen in Alzheimer's disease.[24] Besides, increased concentration of aluminium in the brain has also been observed in neuritic deposits, plaques and neurofibrillay tangles in the brain in Alzheimer's disease. It has been reported that aluminium accumulates significantly in the hippocampus following its chronic exposure. Aluminium gains access to the brain via specific high affinity receptors for transferrin that are expressed in the blood–brain barrier. Upon entering the brain it affects the slow and fast axonal transports, induces inflammatory responses, inhibits long-term potentiation and causes synaptic structural abnormalities, resulting thereby in profound memory loss. At the molecular level, aluminium influences DNA topology, gene transcription and cellular energy metabolism. It induces misfolding and self-aggregation of highly phosphorylated cytoskeletal proteins, such as neurofilaments or microtubule-associated proteins and Aβ, which are implicated in Alzheimer's disease. Besides, induction of aluminium-induced neurotoxicity is known to be safer than other Alzheimer's disease models, which account for higher mortality owing to the surgical intervention for intracerebroventricular administration of neurotoxins.[21,24] Hence, in this investigation, it was decided to induce Alzheimer's disease through oral administration of 100 mg/kg of aluminium chloride.

The results of the spatial navigation test and elevated plus maze paradigm suggest that aluminium chloride caused significant cognitive impairment in rats. However, chronic treatment with quercetin-loaded SLNs in aluminium chloride-treated rats was able to reverse the deleterious neurodegenerative effects of aluminium chloride. Earlier studies report improved efficacy of metal chelators in Alzheimer's disease on being formulated as nanoparticles.[48,49] Nanoparticles, having some metal-chelating activity of their own, also significantly improve the brain permeation of drugs encapsulated in their lipidic matrices. In this study too, the antioxidant potential of quercetin was significantly enhanced by formulating it as SLNs. The results are in consonance with literature where nanoparticles coated with Tween 80 have been employed for brain targeting of a variety of drugs.[50–52] However, in this study, Tween 80 is an integral part of the formulation system. Hence, SLNs without an additional coating of Tween 80 preformed better than those

coated with the surfactant. This was because an additional coating of Tween 80 caused the particles to coalesce, thus increasing their particle size and hindering their entry into the CNS. Further, better regulation of lipid peroxidation, as signified by constant levels of malondialdehyde in rats treated with SLN-encapsulated quercetin vis-à-vis the diseased (test) rats, and maintenance of glutathione and nitrite levels in the brain homogenates, ratified the application of quercetin-loaded SLNs in reversal of aluminium-induced neurotoxicity.

Conclusions

The limited permeability of many therapeutic molecules across the blood–brain barrier can be improved by employing several techniques, like administering them through the intraventricular or intrathecal route or formulating them as nanoparticulate systems. As a lot of patient non-compliance is associated with the intraventricular/intrathecal routes, this study aimed at formulating SLNs of quercetin, a potential antioxidant, to target it to the CNS in the treatment of Alzheimer's disease. It was a Herculean task to attain the required drug entrapment, particle size, zeta potential and drug release characteristics in the formulation using blends of Compritol and Tween 80 because of the diverse nature of these polymers. Only systematic studies using DoE optimization could surmount this hiccup of balancing the response parameters. The choice of experimental design (i.e. a 2-factor CCD) was found to be highly appropriate, as it can detect any non-linearity in factor-response relationship with minimal expenditure of developmental effort and time. The optimized formulation exhibited marked behavioral improvement in memory retention in rats with aluminium-induced dementia. Besides, the maintenance of lipid peroxidation, glutathione and nitrite levels in the brain homogenates of these rats also corroborated successful targeting of quercetin-loaded SLNs into the CNS. Hence, the significant reversal of aluminium-induced neurotoxicity achieved by employing quercetin-loaded SLNs indicates the immense potential of SLNs as a platform technology to target various natural and synthetic molecules to the brain to improve their efficacy in various CNS disorders.

Declarations

Conflict of interest

The Author(s) declare(s) that they have no conflicts of interest to disclose.

Funding

Financial assistance from Indian Council of Medical Research (ICMR), New Delhi is gratefully acknowledged.

Acknowledgements

The authors are thankful to Dr Kanwaljit Chopra and Dr Indu Pal Kaur (UIPS) for providing the requisite facilities to conduct the behavioral studies, and Dr Anil Kumar (UIPS) for helping in the biochemical estimations.

References

1. Behl C. The search for novel avenues for the therapy and prevention of Alzheimer's disease. *Drug News Perspect* 2006; 19: 5–12.
2. Pietrzik C, Behl C. Concepts for the treatment of Alzheimer's disease: molecular mechanisms and clinical application. *Int J Exp Pathol* 2005; 86: 173–185.
3. Mott RT, Hulette CM. Neuropathology of Alzheimer's disease. *Neuroimaging Clin N Am* 2005; 15: 755–765.
4. Dhawan K, Dhawan S. The importance of Passionflower in therapeutics – some folklore medicinal use and the latest pharmacological studies. In: Govil JN, Singh VK, eds. *Recent Progress in Medicinal Plants*. Houstan, USA: Texas: Stadium press, LLC, 2006.
5. Dhawan K *et al*. Passiflora: a review update. *J Ethnopharmacol* 2004; 94: 1–23.
6. Dhawan K *et al*. Attenuation of benzodiazepine dependence in mice by a tri-substituted benzoflavone moiety of Passiflora incarnata Linneaus: a non-habit forming anxiolytic. *J Pharm Pharm Sci* 2003; 6: 215–222.
7. Behl C, Moosmann B. Oxidative nerve cell death in Alzheimer's disease and stroke: antioxidants as neuroprotective compounds. *Biol Chem* 2002; 383: 521–536.
8. Huber A *et al*. Neuroprotective therapies for Alzheimer's disease. *Curr Pharm Des* 2006; 12: 705–717.
9. Rice-Evans CA *et al*. The relative antioxidant activities of plant-derived polyphenolic flavonoids. *Free Radic Res* 1995; 22: 375–383.
10. Hu P *et al*. Quercetin relieves chronic lead exposure-induced impairment of synaptic plasticity in rat dentate gyrus in vivo. *Naunyn Schmiedebergs Arch Pharmacol* 2008; 378: 43–51.
11. Kitagawa S *et al*. Enhanced skin delivery of quercetin by microemulsion. *J Pharm Pharmacol* 2009; 61: 855–860.
12. Wu TH *et al*. Preparation, physicochemical characterization, and antioxidant effects of quercetin nanoparticles. *Int J Pharm* 2008; 346: 160–168.
13. Bondi ML *et al*. Brain-targeted solid lipid nanoparticles containing riluzole: preparation, characterization and biodistribution. *Nanomedicine* 2010; 5: 25–32.
14. Wong HL *et al*. Nanotechnology applications for improved delivery of antiretroviral drugs to the brain. *Adv Drug Deliv Rev* 2010; 62: 503–517.
15. Singh B *et al*. Formulation development of oral controlled release tablets of hydralazine: optimization of drug release and bioadhesive characteristics. *Acta Pharm* 2009; 59: 1–13.
16. Li H *et al*. Enhancement of gastrointestinal absorption of quercetin by solid lipid nanoparticles. *J Controlled Release* 2009; 133: 238–244.
17. Singh B, Singh S. A compreshensive computer program for study of drug release kinetics from compressed matrices. *Indian J Pharm Sci* 1998; 60: 313–316.
18. Singh B *et al*. Correction of raw dissolution data for loss of drug during sampling. *Indian J Pharm Sci* 1997; 59: 196–199.
19. Sashmal S *et al*. Design and optimization of NSAID loaded nanoparticles. *Pak J Pharm Sci* 2007; 20: 157–162.
20. Reagan-Shaw S *et al*. Dose translation from animal to human studies revisited. *FASEB J* 2008; 22: 659–661.
21. Kumar A *et al*. Colchicines-induced neurotoxicity as an animal model of sporadic dementia of Alzheimer's type. *Pharmacol Rep* 2007; 59: 274–283.
22. Hemb M *et al*. Effects of early malnutrition, isolation and seizures on memory and spatial learning in the developing rat. *Int J Dev Neurosci* 2010; 28: 303–307.

23. Skirzewski M *et al*. Acute lecozotan administration increases learning and memory in rats without affecting anxiety or behavioral depression. *Pharmacol Biochem Behav* 2010; 95: 325–330.
24. Kumar A *et al*. Protective effect of curcumin (Curcuma longa), against aluminium toxicity: possible behavioral and biochemical alterations in rats. *Behav Brain Res* 2009; 205: 384–390.
25. Gaur V *et al*. Protective effect of naringin against ischemic reperfusion cerebral injury: possible neurobehavioral, biochemical and cellular alterations in rat brain. *Eur J Pharmacol* 2009; 616: 147–154.
26. Kumar P, Kumar A. Protective effect of rivastigmine against 3-nitropropionic acid-induced Huntington's disease like symptoms: possible behavioural, biochemical and cellular alterations. *Eur J Pharmacol* 2009; 615: 91–101.
27. Daniel WW. *Biostatistics: A Foundation for Analysis in the Health Sciences*. 7th Edition edn. Singapore: John Wiley & Sons, 2000.
28. Kaur IP *et al*. Potential of solid lipid nanoparticles in brain targeting. *J Controlled Rel* 2008; 127: 97–109.
29. Passerini N *et al*. Evaluation of solid lipid microparticles produced by spray congealing for topical application of econazole nitrate. *J Pharm Pharmacol* 2009; 61: 559–567.
30. Hu L *et al*. Preparation and characterization of solid lipid nanoparticles loaded with epirubicin for pulmonary delivery. *Pharmazie* 2010; 65: 585–587.
31. Mulik RS *et al*. Transferrin mediated solid lipid nanoparticles containing curcumin: enhanced in vitro anticancer activity by induction of apoptosis. *Int J Pharm* 2010; 398: 190–203.
32. Blasi P *et al*. Solid lipid nanoparticles for targeted brain drug delivery. *Adv Drug Deliv Rev* 2007; 59: 454–477.
33. Bhalekar MR *et al*. Preparation and evaluation of miconazole nitrate-loaded solid lipid nanoparticles for topical delivery. *AAPS PharmSciTech* 2009; 10: 289–296.
34. Abdelbary G, Fahmy RH. Diazepam-loaded solid lipid nanoparticles: design and characterization. *AAPS PharmSciTech* 2009; 10: 211–219.
35. Singh B, Ahuja N. Development of controlled-release buccoadhesive hydrophilic matrices of diltiazem hydrochloride: optimization of bioadhesion, dissolution, and diffusion parameters. *Drug Dev Ind Pharm* 2002; 28: 431–442.
36. Singh B *et al*. Optimizing drug delivery systems using systematic 'design of experiments.' Part II: retrospect and prospects. *Crit Rev Ther Drug Carrier Syst* 2005; 22: 215–294.
37. Singh B *et al*. Formulation and optimization of controlled release mucoadhesive tablets of atenolol using response surface methodology. *AAPS PharmSciTech* 2006; 7: E1–E10.
38. Singh B, Agarwal R. Design development and optimization of controlled release microcapsules of diltiazem hydrochloride. *Indian J Pharm Sci* 2002; 64: 378–385.
39. Singh B *et al*. Optimizing drug delivery systems using systematic 'design of experiments.' Part I: fundamental aspects. *Crit Rev Ther Drug Carrier Syst* 2005; 22: 27–105.
40. Singh B, Ahuja N. Response surface optimization of drug delivery systems. In: Jain NK, ed. *Progress in Controlled and Novel Drug Delivery Systems*. New Delhi: CBS Publishers, 2004: 470–509.
41. Singh B *et al*. Formulation optimization of hydrodynamically balanced oral controlled release bioadhesive tablets of tramadol hydrochloride. *Sci Pharm* 2010; 78: 303–323.
42. Thakkar H *et al*. Enhanced retention of celecoxib-loaded solid lipid nanoparticles after intra-articular administration. *Drugs R D* 2007; 8: 275–285.
43. Jain SK *et al*. Development and characterization of 5-FU bearing ferritin appended solid lipid nanoparticles for tumour targeting. *J Microencapsul* 2008; 25: 289–297.
44. Tangsuphoom N, Coupland JN. Effect of pH and ionic strength on the physicochemical properties of coconut milk emulsions. *J Food Sci* 2008; 73: E274–E280.
45. Yeung A *et al*. Shear-induced coalescence of emulsified oil drops. *J Colloid Interface Sci* 2003; 265: 439–443.
46. Subedi RK *et al*. Preparation and characterization of solid lipid nanoparticles loaded with doxorubicin. *Eur J Pharm Sci* 2009; 37: 508–513.
47. Hu L *et al*. Preparation and enhanced oral bioavailability of cryptotanshinone-loaded solid lipid nanoparticles. *AAPS PharmSciTech* 2010; 11: 582–587.
48. Liu G *et al*. Nanoparticle and other metal chelation therapeutics in Alzheimer disease. *Biochim Biophys Acta* 2005; 1741: 246–252.
49. Liu G *et al*. Nanoparticle-chelator conjugates as inhibitors of amyloid-beta aggregation and neurotoxicity: a novel therapeutic approach for Alzheimer disease. *Neurosci Lett* 2009; 455: 187–190.
50. Kurakhmaeva KB *et al*. Brain targeting of nerve growth factor using poly(butyl cyanoacrylate) nanoparticles. *J Drug Target* 2009; 17: 564–574.
51. Ren T *et al*. Preparation and therapeutic efficacy of polysorbate-80-coated amphotericin B/PLA-b-PEG nanoparticles. *J Biomater Sci Polym Ed* 2009; 20: 1369–1380.
52. Goppert TM, Muller RH. Polysorbate-stabilized solid lipid nanoparticles as colloidal carriers for intravenous targeting of drugs to the brain: comparison of plasma protein adsorption patterns. *J Drug Target* 2005; 13: 179–187.